

Watershed Delineation On A Hexagonal Mesh Grid

Chang Liao^a, Teklu Tesfa^b, Zhuoran Duan^b, L. Ruby Leung^a

^aAtmospheric Sciences and Global Change, Pacific Northwest National Laboratory,
Richland, WA, USA

^bHydrology Group, Pacific Northwest National Laboratory, Richland, WA, USA

Abstract

Spatial discretization is the cornerstone of all spatially-distributed numerical simulations including watershed hydrology. Traditional square grid spatial discretization has several limitations including inability to represent adjacency uniformly. In this study, we developed a watershed delineation model (HexWatershed) based on the hexagon grid spatial discretization. We applied this model to two different types of watershed in the US and we evaluated its performance against the traditional method. The comparisons show that the hexagon grid spatial discretization exhibits many advantages over the tradition method. We propose that spatially distributed hydrologic simulations should consider using a hexagon grid spatial discretization.

Keywords: Hydrology, Hexagon, Watershed delineation, Digital Global Grid System

1. Introduction

2 Spatial discretization is the cornerstone of all spatially distributed nu-
3 mercial simulations including hydrologic simulations. In hydrologic modeling
4 the study domain is commonly discretized using a Square Grid Spatial Dis-
5 cretization (SGSD). Few studies have investigated the performance of other
6 spatial discretizations such as Hexagon Grid Spatial Discretization (HGSD)
7 in hydrology [35, 33].

8 By definition, spatial discretization is the representation of the continu-
9 ous real world with discrete information. In Geographic Information System
10 (GIS), SGSD is the most widely used approach to represent spatial informa-
11 tion. For example, a raster Digital Elevation Model (DEM) dateset is usually
12 used to describe the surface elevation of a Region Of Interest (ROI) on the

13 Earth's surface [8]. Because SGSD data structure can be represented by a
14 rectangular array /matrix directly, it is convenient for computation, analysis,
15 visualization and storage. However, SGSD has several limitations.

16 First, SGSD cannot represent adjacency uniformly [4]. In a Cartesian
17 coordinate system, each grid has two types of neighbors: direct and diag-
18 onal. The distances between the center of a grid and the center of its diagonal
19 neighbors are further than that of the direct ones (Figure 1a). As a result,
20 hydrologic models have to assign different weights, arbitrarily or empirically,
21 to account for the differences in travel distances. These differences are also
22 not always treated consistently. For example, in a coupled surface and sub-
23 surface hydrologic simulation, water flow in the diagonal direction may be
24 considered in the surface hydrology component whereas it is ignored in the
25 groundwater hydrology component [10, 12, 19, 15]. Consequently, it becomes
26 one of the major model uncertainty sources (input data, model structure and
27 parameters) in hydrologic modeling. In the remainder of the paper, the term
28 "uncertainty" refers to model uncertainty caused by model structure unless
29 otherwise specified. Because the diagonal neighbors are connected through
30 the vertices instead of faces, they cannot represent stream width information
31 correctly (Figure 1a). Similarly, flow width information of the surface runoff
32 is misrepresented.

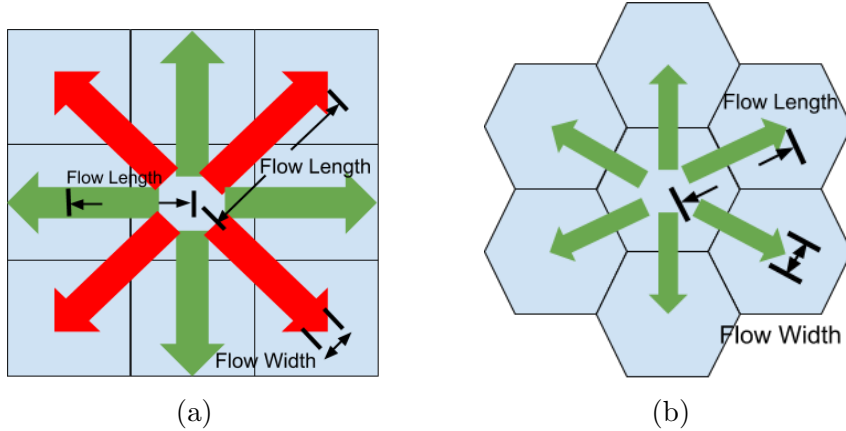


Figure 1: Illustration of traditional D4/D8 neighbor definitions and the hexagonal D6 neighbor definitions. (a) the center square grid have 4 direct/face (green arrows) and 4 diagonal/vertex (red arrows) neighbors; (b) the center hexagon grid has 6 face neighbors (green arrows). The arrows also represent flow path with both length and width information. In D4/D8, diagonal flow length is longer than direct flow length, and flow width is out of boundary. In hexagonal D6, flow length is the same and flow width is within boundary.

Second, SGSD will create “island” effect due to the differences in D4 and D8 neighbor definitions, which causes problems for numerical simulations [3]. In this study, we define a single or group of grids that are connected through diagonal path at the edge of boundaries as an island. For this reason, watershed delineation results usually require tedious manual correction to eliminate these diagonal islands between subbasin boundaries [14]. Besides, because most groundwater flow models do not consider D8 neighbors, we cannot couple them with surface hydrology models directly [10, 19]. For example, we need to set the grid #1 as inactive in a coupled Groundwater and Surface Water Flow Model (GSFLOW) simulation (Figure 2) [18].

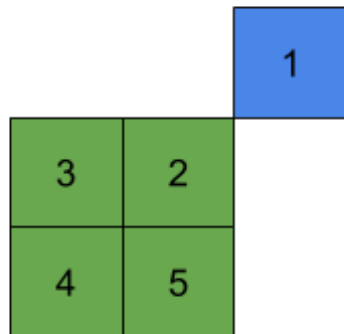


Figure 2: Illustration of “island” effect caused by D8 diagonal neighbor definition. The blue grid (#1) is a D8 diagonal neighbor of the green grid (#2). This blue grid can occur either within model domain or at the edge [14].

43 Third, SGSD cannot effectively represent a spherical topology, which will
 44 introduce significant spatial distortions (Figure 3). Hydrologic simulations
 45 at global scale that use longitude/latitude mesh grid will be undermined,
 46 especially when the ROI is also the most distorted areas. For this reason,
 47 longitude/latitude based river routing models (e.g., MOdel for Scale Adap-
 48 tive River Transport (MOSART)) may contain larger uncertainty at high
 49 latitudes [24, 16]. Furthermore, as global scale oceanic models do not use
 50 SGSD method, it becomes cumbersome to couple land surface/hydrologic
 51 models with oceanic models.

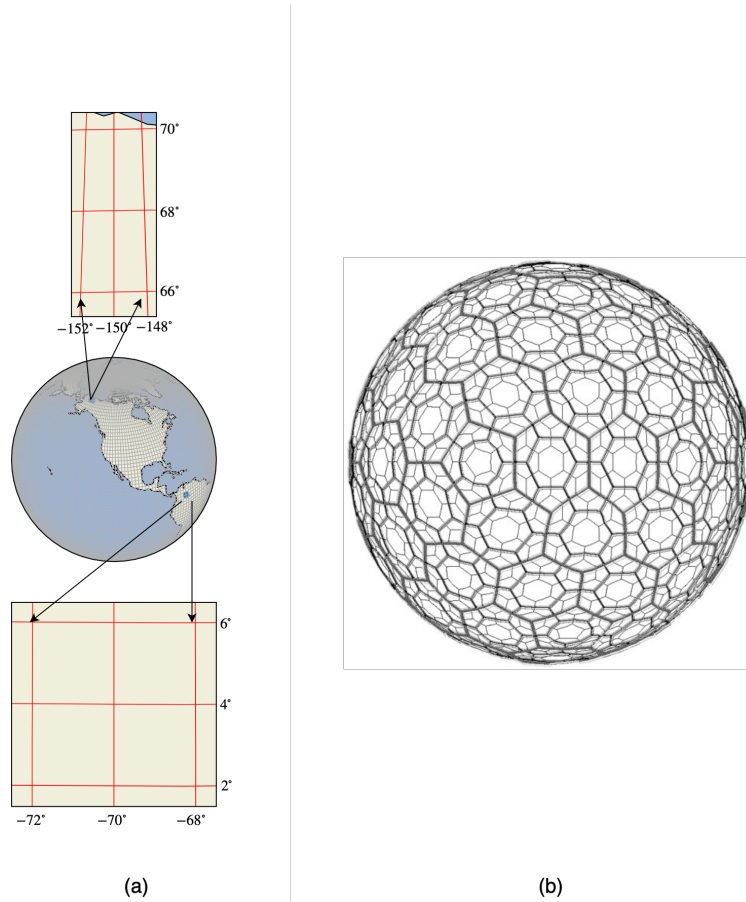


Figure 3: Illustration of the spatial distortion caused by longitude/latitude based SGSD method and a Discrete Global Grid System (DGGS) with uniform resolution. (a) is a longitude/latitude mesh at $2^\circ \times 2^\circ$ resolution. The ratio of distance in latitude to longitude increases with latitude. Top and bottom plots in (a) are zoom-in regions in Alaska, USA, and east Columbia. Their corresponding ratios are close to 2.5 and 1.0, respectively. (b) is a DGGS grid generated by DGGRID, which is made up by mostly hexagons [25]¹. All the hexagons have nearly the same resolution.

52 Other flow direction methods based on the SGSD also have similar limit-
 53 tations. For example, the D-infinity flow direction method can describe the
 54 flow direction in 360° and improve the partition of water flow in different di-
 55 rections [28]. However, these methods do not resolve the SGSD limitations

¹There are 12 pentagons.

56 fundamentally and they are relatively less used in hydrologic simulations.

57 Triangular irregular networks (TIN) Spatial Discretization (TINSD) is
58 also used in hydrologic models. One advantage of the TINSD method is that
59 points of a TIN are distributed variably so it can provide high resolution near
60 ROI whereas low resolution elsewhere [7]. However, this method is less popu-
61 lar because of the complex data structure. Because it has two types of neigh-
62 bor connectivity (3 face neighbors and multiple vertice neighbors), it may
63 also introduce uncertainty. For example, the Penn State Integrated Hydro-
64 logic Model (PIHM) only considers water flow through the face neighbors but
65 ignores the vertice neighbors [22]. Hereafter, our discussion excludes TINSD
66 unless otherwise specified. Watershed boundary-based spatial discretization
67 (WBSD) is also used in large scale hydrologic simulations [30, 31]. However,
68 this method essentially depends on the availability of watershed boundaries,
69 which mostly come from SGSD based watershed delineation processes.

70 In contrast, the HGSD method can resolve these limitations:

- 71 1. In HGSD, each grid has only one type of neighbor with the same con-
72 nectivity and distance (Figure 1b). As a result, we can route both
73 surface and subsurface water flow consistently without using different
74 weights, thus getting rid of the decadal old assumption on travel length.
75 This will improve spatially distributed hydrologic models that rely on
76 grid connectivity [17].
- 77 2. The “island” effect is automatically eliminated because all neighbors
78 are connected through faces. No manual corrections are needed to
79 resolve the diagonal traveling path issue [14].
- 80 3. It can provide continental to global coverage at consistent or variable
81 spatial resolutions (Figure 3b) [26]. It can be used to couple land
82 surface/hydrologic models with oceanic models using a unified mesh
83 grid (e.g., the Voronoi tessellation of the Model for Prediction Across
84 Scale (MPAS)) [5].

85 Additionally, it has other advantages:

- 86 1. It can be used for coupled surface (D6) and subsurface (9-point struc-
87 tured connectivity) hydrologic modeling to resolve the inconsistency in
88 connectivity.
- 89 2. The conceptual model is more compatible with the flow width informa-
90 tion because the flow path can be contained within the grid boundary
91 (Figure 1b).

- 92 3. It can improve model performance as many studies show that numerical
 93 simulations based on hexagon grid perform better when compared with
 94 other mesh grids [4, 35, 34, 9].
 95 4. Other flow direction methods (e.g., D-infinity) can also be implemented
 96 on HGSD with modifications to improve flow direction and partitions
 97 [28].

98 In recent decades, HGSD is widely used in Discrete Global Grid System
 99 (DGGS) [35, 23]. For example, the Icosahedral Snyder Equal Area (ISEA)
 100 tessellation method is used to generate a geodesic grid system within which
 101 most grids can be hexagons [26].

102 Despite all the advantages the HGSD method can provide, it is not widely
 103 used in numerical simulations. Partially it is because most existing datasets
 104 were generated in the SGSD format and numerical models were not designed
 105 to use the HGSD datasets. For example, nearly all the spatially distributed
 106 hydrologic models were developed based on square or unstructured grid dis-
 107 cretization, and very few studies have used HGSD.

108 In this study, we made the first attempt to develop a watershed delin-
 109 eation model (HexWatershed) with a set of algorithms based on the HGSD
 110 method. In Section 2 we introduce the model algorithms. In Section 3 we
 111 apply the model to two different types of watersheds and analyze the model
 112 outputs. In Section 4 we evaluate the model performance against outputs
 113 from the traditional SGSD method. In Section 5 and 6 we discuss the limi-
 114 tations and future work.

115 2. Model Algorithm

116 2.1. Overview

117 Following the traditional watershed delineation algorithms, we developed
 118 a list of algorithms for the HGSD method. Because these algorithms are fun-
 119 damentally similar in principle, we mainly focus on the differences that were
 120 introduced in the new model. Last, we describe the software requirements
 121 to run the HexWatershed model.

122 2.2. Hexagon Grid Resolution

123 The hexagon grid resolution is defined using grid area instead of edge
 124 length so it is comparable with the traditional square grid [33]. For example,
 125 if the edge length of a hexagon is 10 m, its area is approximately 259.81m²,

126 then its equivalent/effective square grid resolution is 16.11 m, which is the
127 square root of its area (Equation 1 and 2).

$$A = \frac{3 \times \sqrt{3}}{2} L^2 \quad (1)$$

$$R_e = \sqrt{A} \quad (2)$$

129 where A is the hexagon area; L is the actual hexagon edge length; and R_e is
130 the effective hexagon resolution.

131 Although applications of HexWatershed in this study use a constant reso-
132 lution hexagonal mesh (Section 3), it also supports variable resolution hexag-
133 onal mesh. All algorithms within HexWatershed are designed and imple-
134 mented independent of resolution. For example, the stream grid algorithm
135 considers the total drainage area because area of each hexagon grid may be
136 different (Section 2.9).

137 2.3. Grid Topology

138 In SGSD, grid is often referred by its array/matrix indices (i, j) and its
139 neighbors can be referred by moving up/down the indices $(i \pm 1, j \pm 1)$.
140 However, in HGSD, we cannot use array indices directly unless a dedicated
141 hexagon grid index system is available [27]. As a result, an algorithm is
142 required to obtain the topology. Depending on how the hexagon grid was
143 generated, there are different ways to obtain the grid topology.

144 For the sake of generality, we assume that there is no prior grid topology
145 stored within the hexagon grid. HexWatershed rebuilds the topology with
146 three steps:

- 147 1. Assign a unique global ID for each hexagon;
- 148 2. For each hexagon, identify hexagons that share the same vertex/edge
149 as neighbors; and
- 150 3. Save the global IDs of these neighbors into a look-up table for each
151 hexagon.

152 The final look-up table of this algorithm is illustrated in Figure 4.

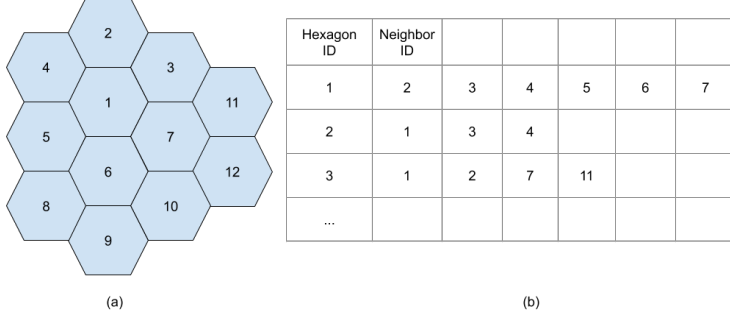


Figure 4: Illustration of hexagon topology. The indices are hexagon grid global IDs. (a) is a hexagon grid; and (b) is the look-up table which stores the hexagon topology. Each hexagon can have a maximal of 6 neighbors.

153 2.4. DEM Resampling

Similar to traditional raster datasets that use grid center to store information, HexWatershed uses the hexagon center to store elevation.

Theoretically, hexagonal DEM can be obtained by resampling from either high resolution traditional DEM, or high resolution hexagonal DEM. In this study, the former approach was used because most available DEM datasets are stored in the SGSD format. To further simplify this process, the nearest neighbor resampling method is used.

161 2.5. DEM Depression Filling

Similar to traditional DEM, hexagonal DEM could potentially have local depressions when generated. We developed an algorithm following the method proposed by Richard Barnes, which uses the priority-flood method to fill the depressions in any grid system [2]. Priority-flood is an efficient algorithm to fill DEM depressions by sequentially “flooding” the domain from the boundary inward to adjust elevations to assure that surface will drain [21]. To ensure an absolute drain, a minimal slope (0.01 in percentage) is added when applicable [32]. The step-by-step instructions are provided in Appendix B and illustrated in Figure 5.

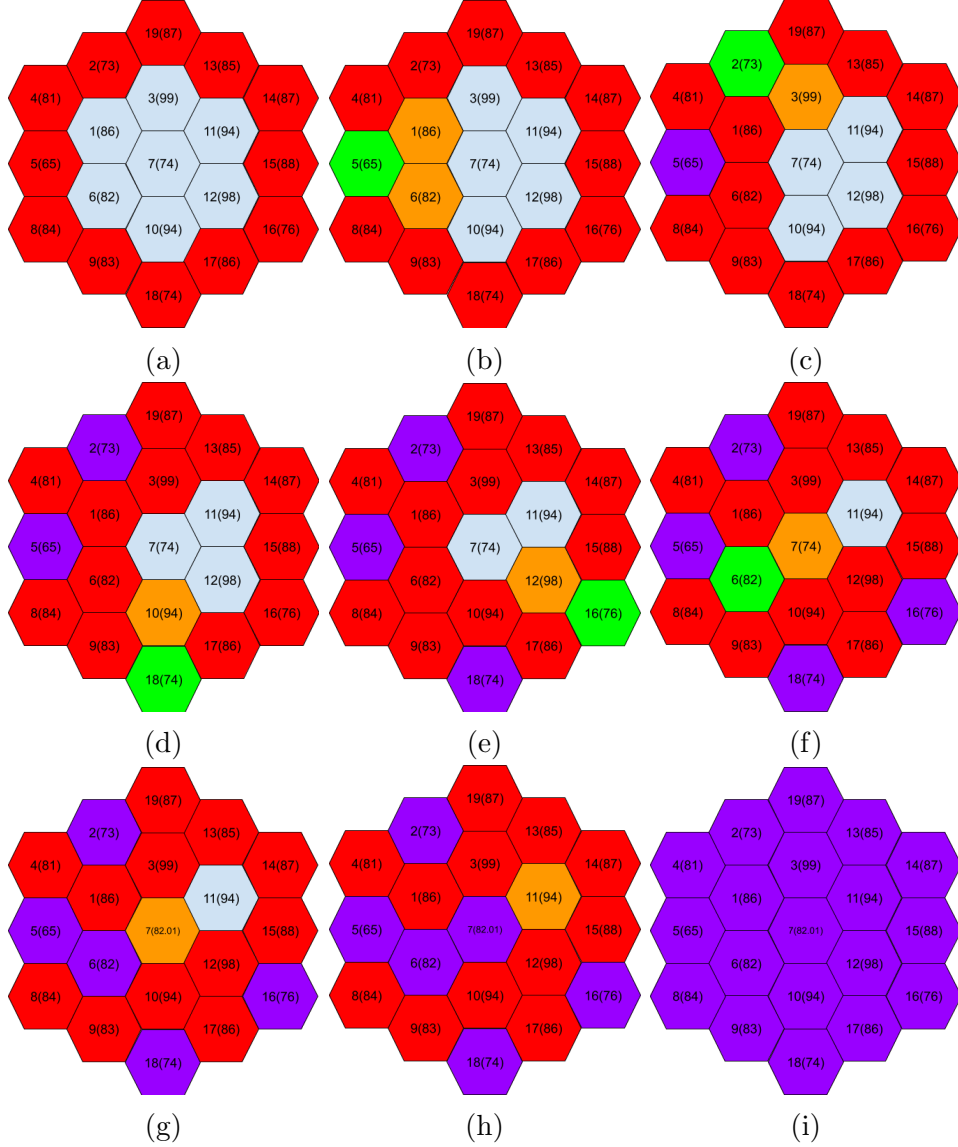


Figure 5: Illustration of the priority-flood depression filling for the HGSD method. Light blue grids represent the initial default state; red grids represent the boundary; green grids represent the to-be-removed grid from the queue; orange grids represent the to-be-added grids into the queue; and purple grids are finished grids. Numbers within each grid represent its global ID and elevation (in parentheses, unit: m), respectively. The algorithm gradually “floods” the domain using a boundary queue (red). If a to-be-added grid has equal or smaller elevation than a to-be-removed grid, its elevation is increased. For example, the elevation of grid #7 is increased from 74 to 82.01 in (g). The step-by-step instructions are provided in [Appendix B](#).

171 *2.6. Flow Direction*

172 Flow direction is defined from the hexagon center to the center of neighbor
173 hexagon which has the lowest elevation. In other words, flow direction is
174 the flow path which has the steepest slope. The global ID of this downslope
175 neighbor is stored in an attribute table. Unlike the traditional SGSD method
176 that uses indices (1, 2, 4, 8, etc.) to represent flow direction, HexWatershed
177 currently represents the flow direction using a flow routing map.

178 *2.7. Flow Accumulation*

179 We developed a flow accumulation algorithm based on the concept from
180 ArcGIS flow accumulation [29]. In short, this algorithm scans all the hexagon
181 grids and sums up the accumulations once all the accumulations of ups-
182 lope hexagons are calculated. It runs recursively until accumulations of all
183 hexagons are calculated (Figure C.17).

184 The flow accumulation algorithm also provides the option to consider
185 variable resolution hexagonal mesh.

186 *2.8. Watershed Boundary*

187 The hexagon grid that has the highest flow accumulation is defined as the
188 watershed outlet. This algorithm scans all the hexagon grids and identifies
189 all the hexagons that contribute to this outlet using the flow routing map.
190 Among them, those at the edge with less than 6 neighbors are used to define
191 the watershed boundary.

192 *2.9. Stream Grid*

193 A hexagon grid is defined as a stream grid if its total drainage area exceeds
194 the minimal drainage area threshold. For a constant resolution hexagonal
195 mesh, each grid's drainage area is proportional to its accumulation value. For
196 a variable resolution hexagonal mesh, each grid's drainage area is summarized
197 from its upslope grids plus its own area.

198 In HexWatershed, a stream grid is also named a “stream reach”, which
199 makes up a stream segment (Section 2.11 and Figure 6).

200 *2.10. Stream Confluence*

201 Stream confluentes are defined based on the flow routing map and stream
202 grids. In short, if a hexagon grid is a stream grid and it has multiple upslope
203 stream reaches, it is defined as a stream confluence. In rare scenarios, a
204 stream confluence may have three or more upslope stream reaches.

205 *2.11. Stream Networks*

206 In HexWatershed, a stream segment is defined as the stream component
207 between headwater/outlet and confluence or between two confluences.

208 To maintain the ascending order from upstream to downstream, we de-
209 veloped an algorithm to define the stream segments reversely from watershed
210 outlet to headwaters.

211 Starting from the watershed outlet, the algorithm searches for stream
212 confluence following the stream grids. Once a stream confluence is found,
213 all of its upslope stream reaches are identified, and the algorithm continues
214 to search recursively until all stream segments are identified. This algorithm
215 works in the following steps:

- 216 1. Calculate the total number (N) of stream segments based on stream
217 confluences information;
- 218 2. Set current outlet and current segment index as the watershed outlet
219 and N , respectively;
- 220 3. Starting from the current outlet, search upstream and assign the cur-
221 rent segment index to each stream reach;
- 222 4. If a confluence is found, set the current outlet and current segment
223 index as this confluence and $N = N - 1$, respectively;
- 224 5. Repeat step 3 and loop through all the upstream segments of this con-
225 fluence;
- 226 6. Stop until all confluences and segments are treated ($N=1$).

227 At the end of this algorithm, a stream segment is made up of a list of
228 stream reaches which have the same segment index. The topology infor-
229 mation of these stream reaches within each stream segment is also defined
230 (Figure 6).

231 *2.12. Stream Topology*

232 Stream topology is defined based on the stream reaches information. If
233 the first stream reach of a stream segment does not have a positive or valid
234 upstream segment index, this stream reach is headwater (Reach #1 in Figure
235 6). Similarly, the segment index (Segment #6) of the downstream of the last
236 stream reach (Reach #3) of a stream segment (Segment #5) is a downstream
237 of Segment #5. Details of stream topology are explained in Figure 6.

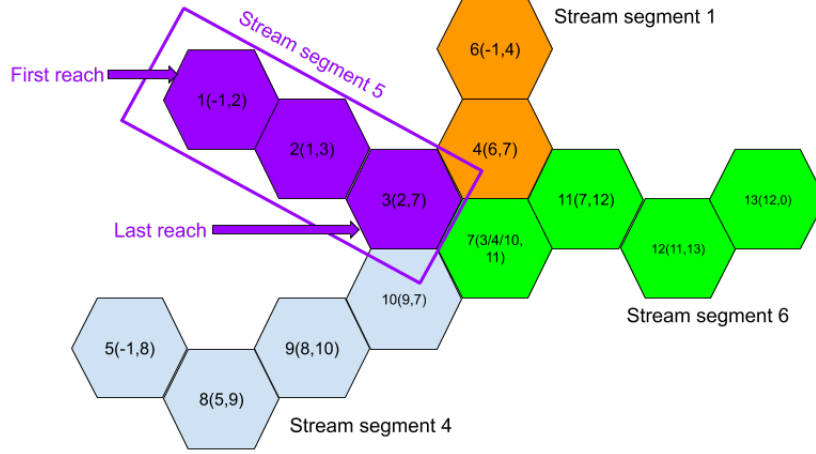


Figure 6: Illustration of the stream topology. Different colors represent 4 different stream segments, respectively. Each stream segment is made up by several stream reaches. For example, the purple stream segment #5 is represented by 3 stream reaches. Numbers with each stream reach represent global ID, upslope and downslope grids global IDs, respectively. Grid #1 and #3 are the first and last reaches of stream segment #5, respectively. Grid #1 does not have upslope stream reach grid and is a headwater. Grid #7 is a confluence and it receives inflow from grid #3, #4 and #7. Therefore stream segment #5 and #6 have a upstream-downstream topology relationship.

238 A stream segment always has only one downstream segment, but it may
 239 have multiple upstream segments unless it is headwater. Besides, both stream
 240 segment indices and stream reach indices within the same segment have as-
 241 cending orders.

242 2.13. Stream Order

243 Stream order is defined following the classical stream order definition [29].
 244 First the stream order of all the headwater stream segments are defined as
 245 1. Then the stream orders of remaining stream segments are defined based
 246 on stream topology.

247 2.14. Subbasin Boundary

248 Similar to stream networks, subbasins are defined reversely. The algo-
 249 rithm works as follows:

- 250 1. Set the last stream segment and watershed outlet as the current stream
 251 segment index N and outlet, respectively;

- 252 2. Scan all the grids that contribute to the current outlet based on the
253 flow routing map, set their subbasin indices to N;
254 3. Go to stream segment $N = N - 1$, repeat step 2;
255 4. Stop until all stream segments are treated (N=1).

256 *2.15. Software Requirements and File I/O*

257 HexWatershed was written in C++11 with OpenMP enabled. It can be
258 applied to both regional and global scales. It is platform independent and
259 parallel computing ready for high performance computing (HPC) [1].

260 To run the HexWatershed model, the minimal software requirements in-
261 clude:

- 262 1. GNU Compiler Collection (GCC) 4.9 and above; and
263 2. Geospatial Data Abstraction Library (GDAL 2.3).

264 The required model inputs include: (a) a high resolution traditional DEM
265 raster file; and (b) a corresponding hexagonal mesh file, which can be gener-
266 ated by any mesh generator. In our study, we used the QGIS MMQGIS plu-
267 gin. The input data must be prepared with the same spatial reference/map
268 projection.

269 After a successful model simulation, HexWatershed produces a list of
270 products including flow direction and stream networks. These products have
271 the same spatial reference as the input data.

272 Because currently a standard file format for HGSD datasets is unavailable,
273 all the model inputs and outputs are stored using the ESRI Shapefile format
274 [6].

275 **3. Application**

276 *3.1. Study Area*

277 To test the performance of HexWatershed model, we applied the model
278 to two different types of watersheds in the western US. Specifically, a moun-
279 tainous area watershed and a flat area watershed are used to demonstrate the
280 capability of HexWatershed model. Then we analyzed the model outputs.

281 The Tin Pan (TP) watershed is located near the northern border of New
282 Mexico. This is a mountainous area watershed with relatively high average
283 surface slope (Figure 7).

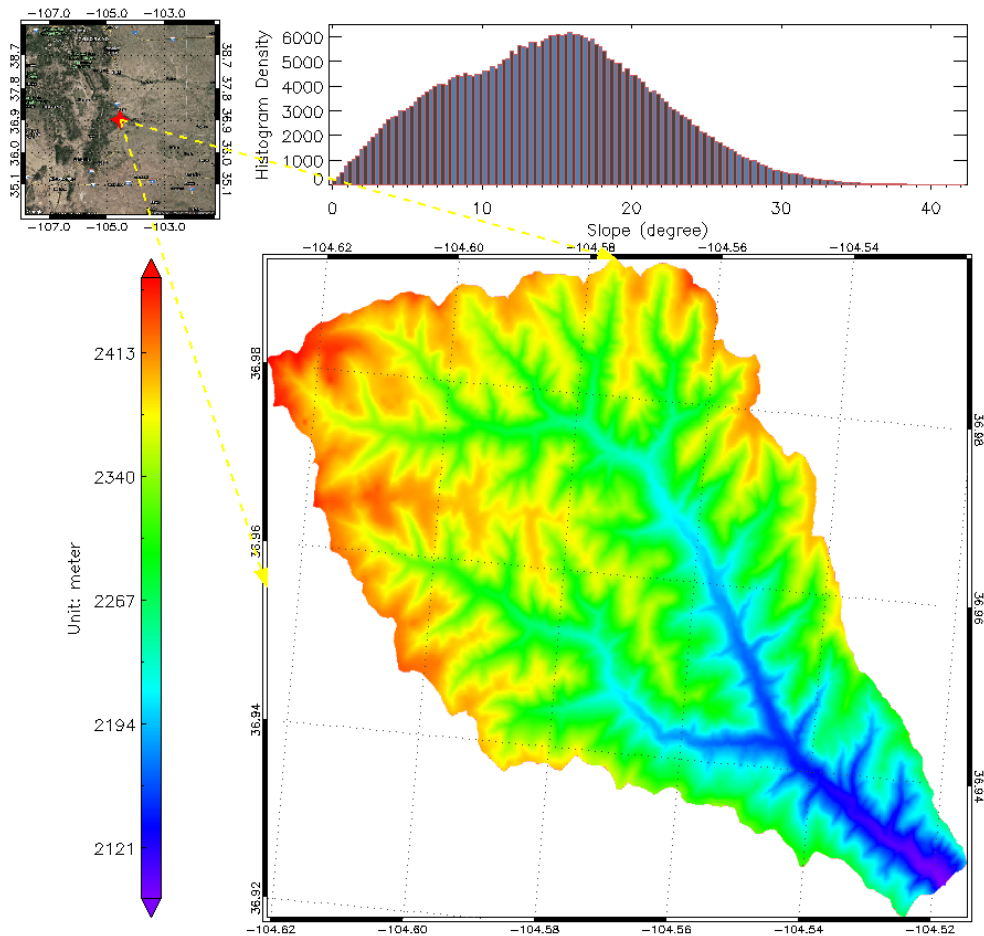


Figure 7: The spatial location, surface elevation and slope distribution of the Tin Pan watershed. Upper left is the location on Google Map; Upper right is the histogram of surface slope (degree); and bottom is the spatial distribution of surface elevation (m).

284 The Columbia Basin flat (CBF) watershed is located near the Columbia
 285 River, Washington. This is a flat area watershed with relatively low average
 286 surface slope (Figure 8).

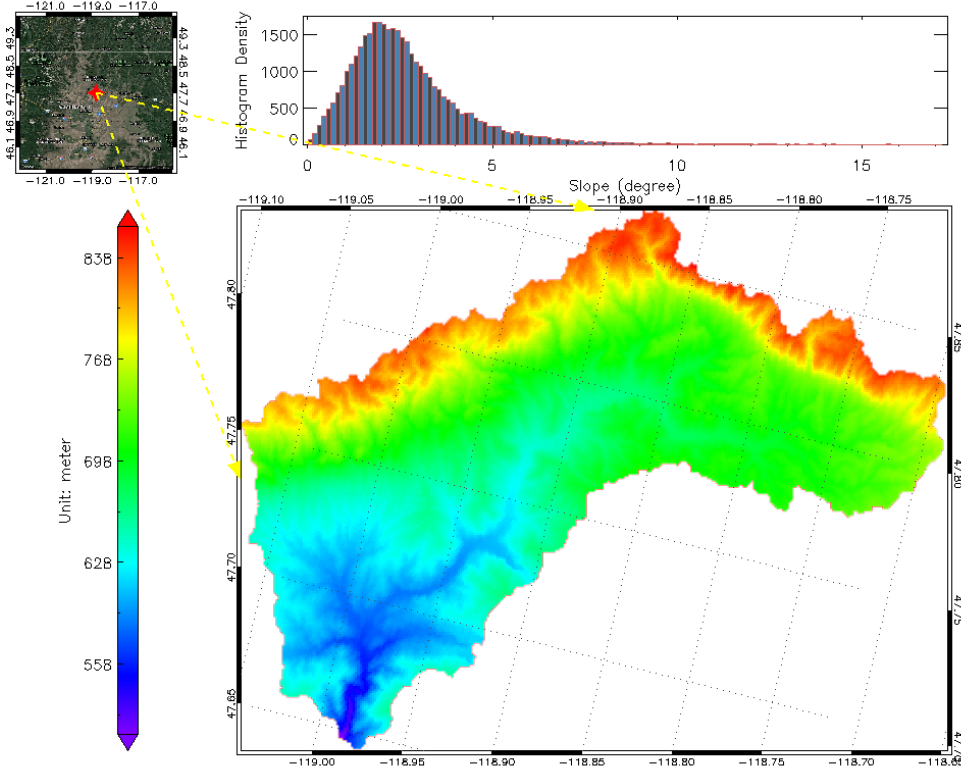


Figure 8: The spatial location, surface elevation and slope distribution of the CBF watershed. Upper left is the location on Google Map; Upper right is the histogram of surface slope (degree); and bottom is the spatial distribution of surface elevation (m).

287

Characteristics of the two watersheds are listed in Table 1.

Table 1: Characteristics of Tin Pan and Columbia Basin flat watersheds.

	TP	CBF
Location (lon, lat)	(-104.52, 36.94)	(-118.82, 47.74)
Elevation range (m)	2091 to 2457	510 to 859
Average slope (degree)	14.66	2.66
Total drainage (km^2)	42	308

288 *3.2. Model Setup*

289 First, we collected raster DEM for both Tin Pan (10 m resolution) and
290 Columbia Basin flat (90 m resolution) watersheds. Then, we generated the
291 hexagonal mesh files for Tin Pan (30 m resolution) and Columbia Basin flat
292 (90 m resolution) watersheds. Last, we ran the HexWatershed model for both
293 watersheds.

294 *3.3. Results*

295 Because of the unique structure, we mainly use visualization to present
296 the model outputs. To provide a clear view of the data structure, we provide
297 zoom-in views of the whole datasets. And the full views of these datasets are
298 provided in [Appendix D](#).

299 *3.3.1. Tin Pan*

300 Zoom-in views (upper left) of model outputs in the Tin Pan watershed
301 are illustrated in Figure [9](#).

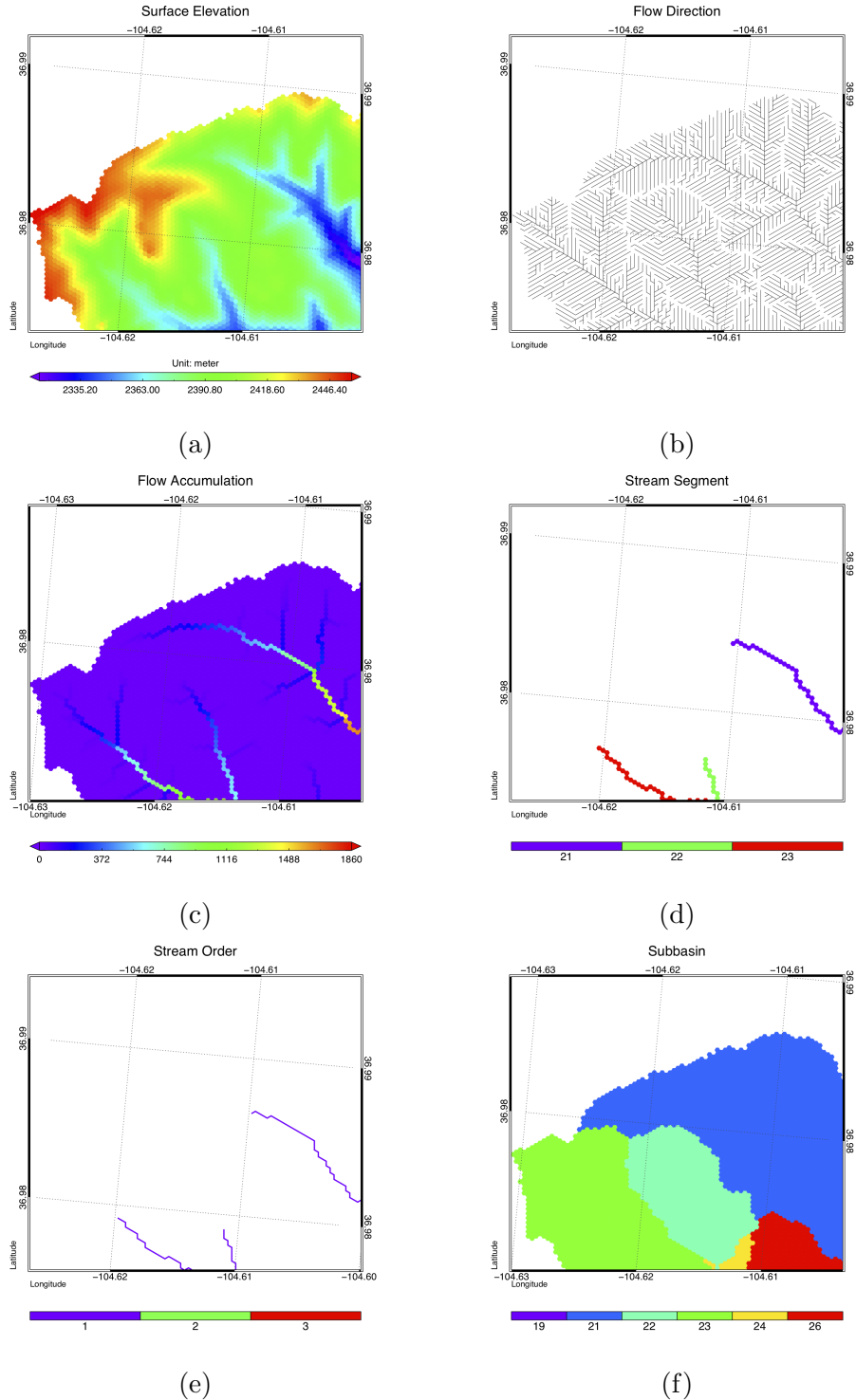


Figure 9: The zoom-in spatial distributions of model outputs in the Tin Pan watershed. (a) is the depression filled hexagonal DEM; (b) is the flow routing; (c) is the flow accumulation; (d) is the stream segments with indices; (e) is the stream order; and (f) is the subbasin with indices.

302 These results show that HexWatershed is able to produce all the traditional
303 watershed delineation characteristics.

304 *3.3.2. Columbia Basin Flat*

305 Zoom-in views (lower left) of model outputs in the Columbia Basin flat
306 watershed are illustrated in Figure 10.

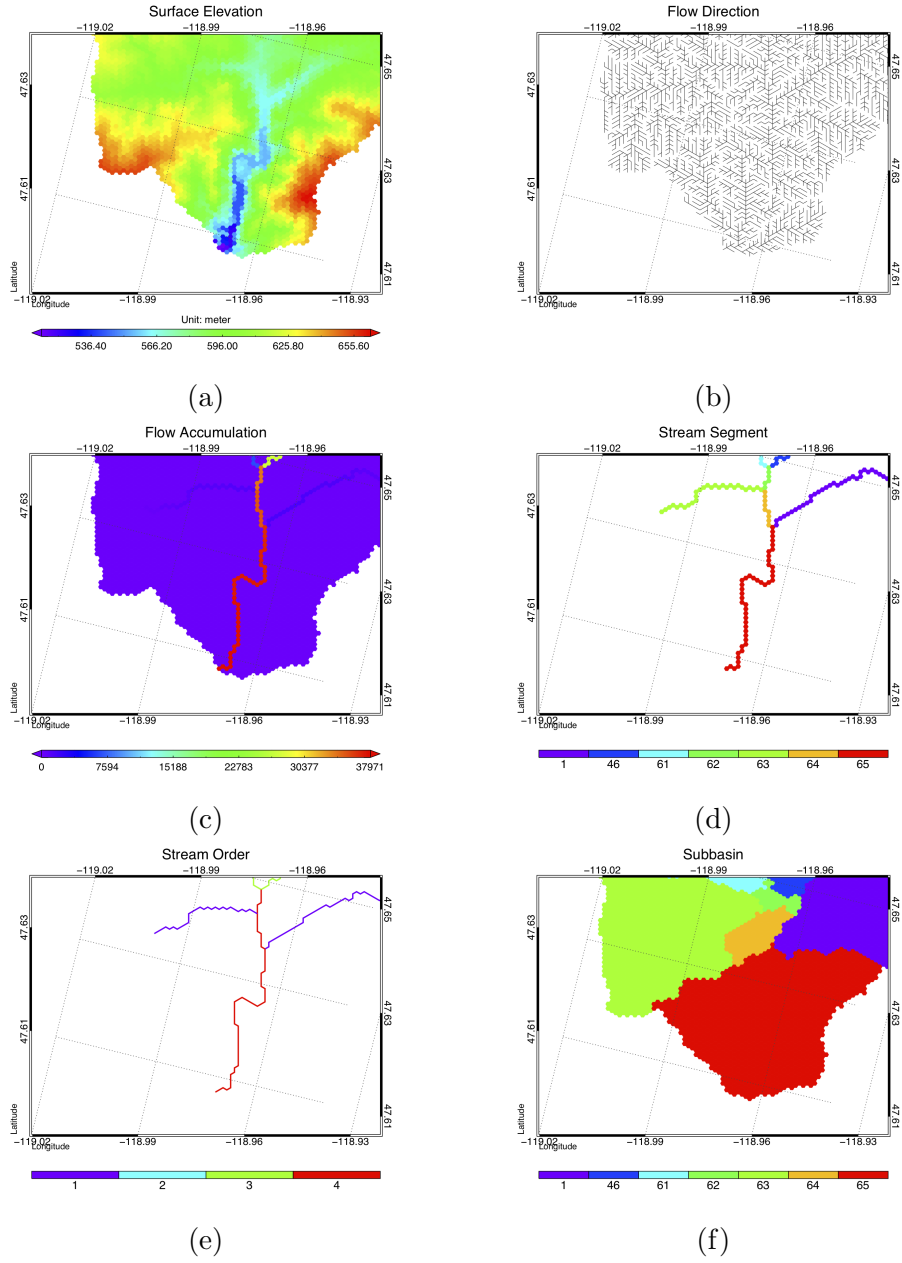


Figure 10: The zoom-in spatial distributions of model outputs in the Columbia Basin flat watershed. (a) is the depression filled hexagonal DEM; (b) is the flow routing; (c) is the flow accumulation; (d) is the stream segments with indices; (e) is the stream order; and (f) is the subbasin with indices.

307 Simulation results from the Columbia basin flat watershed demonstrate
308 that HexWatershed is robust in basins with flat terrain.

309 **4. Comparisons**

310 To evaluate the performance of the HexWatershed model, we compared
311 the model outputs against outputs from the traditional SGSD method.

312 To produce the traditional watershed delineation characteristics, we used
313 the ArcSWAT watershed delineation tool. ArcSWAT is an ArcGIS extension
314 for the Soil & Water Assessment Tool (SWAT), which is widely used in basin
315 scale hydrologic simulations [20, 36].

316 Although HexWatershed is able to produce all the watershed delineation
317 characteristics, we only compared characteristics that are commonly used in
318 hydrologic simulations. Because HexWatershed is robust in different water-
319 sheds, we mainly provide comparison in the Tin Pan watershed and show
320 only selected results from the Columbia Basin flat watershed. To evaluate
321 the sensitivity of HexWatershed to mesh resolution, we ran an addition sim-
322 ulation at Tin Pan watershed using a 100 m resolution hexagonal mesh.

323 *4.1. Hexagonal DEM*

324 The depression filled hexagonal DEM (Figure 9a) has the same spatial
325 pattern as the traditional DEM (Figure 7), and it fits the land surface rea-
326 sonably well.

327 *4.2. Flow Direction*

328 Because HexWatershed does not use indices (1, 2, 4, etc.) to represent
329 flow direction, we cannot compare its flow direction against ArcSWAT flow
330 direction output directly.

331 *4.3. Flow Accumulation*

332 The spatial patterns of flow accumulation from ArcSWAT and HexWa-
333 tershed are similar. However, their spatial distributions are different. For
334 example, ArcSWAT produces more grids with accumulation value at 1, 2
335 and 3 whereas HexWatershed produces more between 4 and 10 (Figure 11).
336 Because of this, HexWatershed produces less spatial variability in flow accu-
337 mulation.

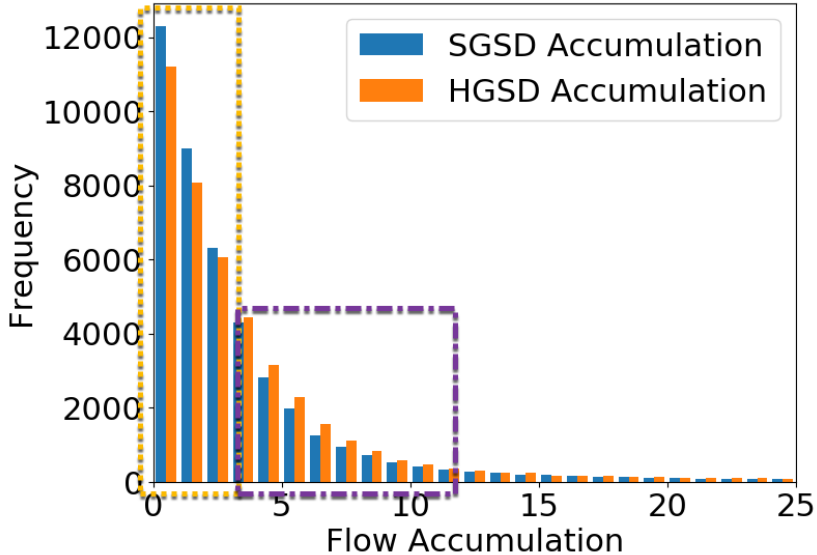


Figure 11: Histograms of flow accumulation from ArcSWAT (SGSD) and HexWatershed (HGSD), respectively. Yellow rectangle features where ArcSWAT produces more grids with accumulation at 1, 2 and 3. Purple rectangle features where HexWatershed produces more grids with accumulation between 4 and 10.

338 *4.4. Subbasin Boundary*

339 ArcSWAT produces diagonal travel path at the subbasin interfaces. For
 340 example, grids with circles are defined within Subbasin #17 when grids with
 341 accumulation 0, 1, 2, and 3 should be in either Subbasin #11 or #12 (Figure
 342 [12a](#)).

343 Meanwhile, HexWatershed is able to eliminate the diagonal travel path,
 344 and the corresponding hexagon grids are clearly defined within Subbasin #2
 345 [2](#) (Figure [12b](#)).

²Because ArcSWAT and HexWatershed use different index systems, subbasin indices are different.

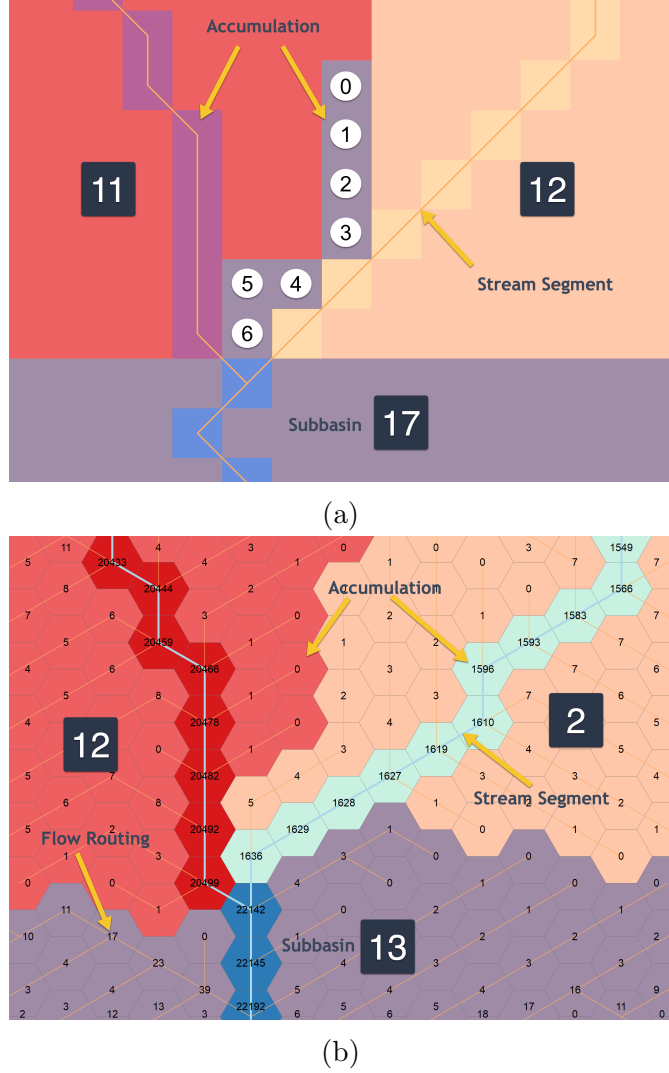


Figure 12: Comparison of flow accumulation and subbasin boundary between model outputs from ArcSWAT and HexWatershed at the same location. (a) are the outputs from ArcSWAT. Square grids with indices represent subbasin. Circles with indices represent flow accumulation. Line features represent stream networks. Because circles from 0 to 6 are connected through diagonal flow path, they are defined in Subbasin #17. (b) are model outputs from HexWatershed. Each hexagon is labelled with its accumulation. Yellow lines between hexagon grids are flow paths.

346 *4.5. Stream Networks*

347 Stream networks produced by HexWatershed are very close to the Arc-
 348 SWAT produced stream networks. To further compare the differences, we
 349 calculated the enclosed area of differences between modelled stream networks
 350 and the National Hydrography Dataset (NHD) flowline datasets. We treat
 351 the NHD flowline as the “true” flow path. In theory, the smaller the total
 352 enclosed area is, the closer the stream networks are to the NHD flowline. To
 353 test the robustness, we compared model outputs at different spatial resolu-
 354 tions. (Figure 13 and Table 2).

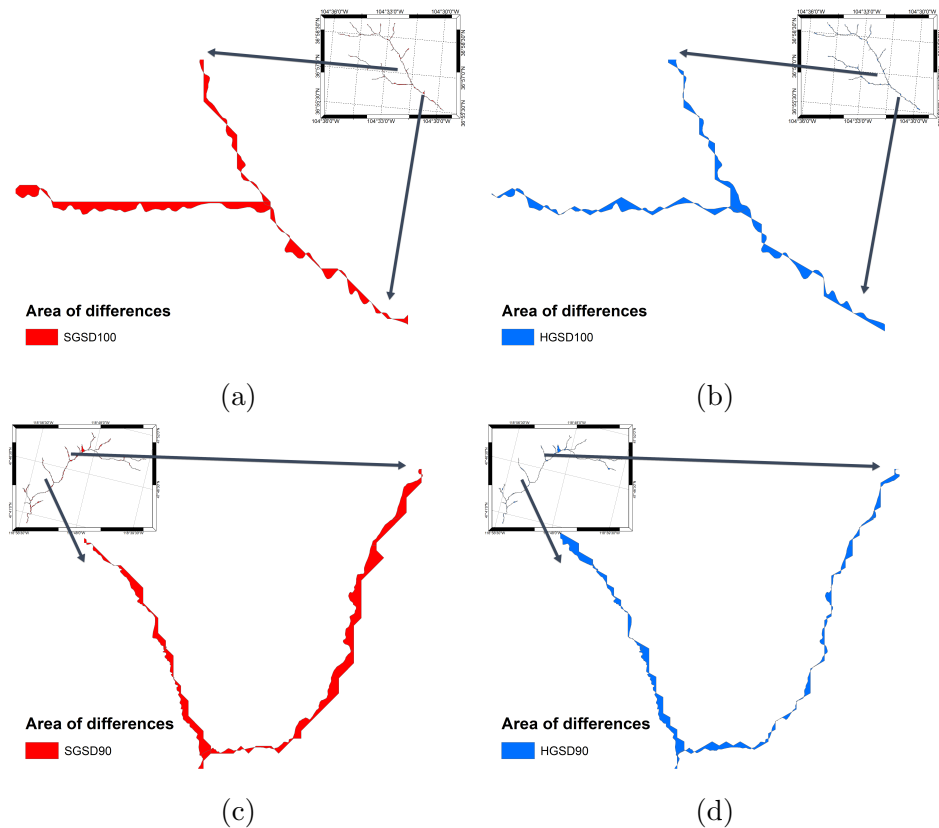


Figure 13: Comparisons of stream networks through enclosed area of differences. These polygons were generated by connecting the NHD flowline with the modelled stream networks. (a) and (b) are areas of differences for ArcSWAT and HexWatershed at 100m resolution in the Tin Pan watershed, respectively. (c) and (d) are areas of differences for ArcSWAT and HexWatershed at 90m resolution in the Columbia Basin flat watershed, respectively.

355 Statistics of areas of differences due to changing spatial resolutions are
 356 provided in Table 2. These statistics show that HexWatershed performs much
 357 better at coarse resolutions.

358 5. Discussion

359 Based on model outputs and comparisons, HexWatershed can provide
 360 equivalent and potentially even better performance than the traditional method.
 361 Because of the close relationship between watershed delineation and surface
 362 hydrology, most hydrologic processes will be affected. Because we didn't
 363 present results on a sphere, our discussion will focus on watershed scale only.

364 First, HexWatershed has successfully eliminated the “island” effect and
 365 tedious manual corrections are no longer needed. Because both subbasin
 366 boundary and watershed boundary are improved, stream discharge in hydro-
 367 logic simulations will be improved (Figure 14).

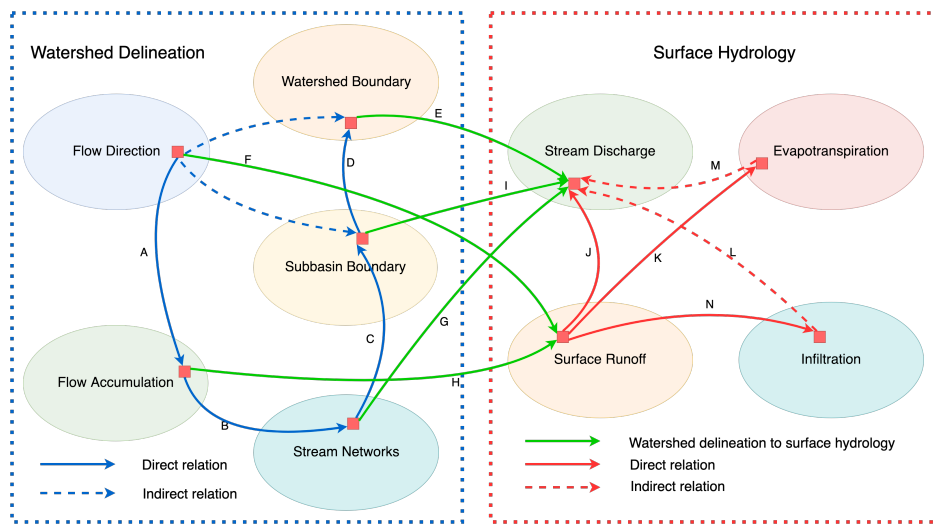


Figure 14: The relationship between watershed delineation and surface hydrology. Circles are major watershed delineation characteristics (left) and hydrologic processes (right). Blue lines show the relationships between watershed characteristics, red lines show the relationships between hydrologic processes, and green lines show the relationships between watershed characteristics and hydrologic processes. The arrows of the lines indicate the direction of influence.

368 Second, although we didn't compare flow direction directly, which es-
 369 sentially determines flow accumulation, and subsequently stream networks,

Table 2: Statistics of areas of differences of stream networks for both 30m and 100m spatial resolutions (m^2).

Watershed	Method with resolution	Mean	Maximum	Sum	Standard Deviation
Tin Pan	SGSD30	554.85	8387.66	225270.04	891.68
	HGSD30	821.74	14328.59	296649.35	1457.44
	SGSD100	3027.82	53887.28	593453.52	4961.07
	HGSD100	2779.15	17059.82	589181.20	2959.10
CBF	SGSD90	25024.08	422748.00	4679503.03	50613.98
	HGSD90	10855.88	504569	3528163.97	33022.46

370 subbasin boundary, it is potentially improved because the latter ones are
371 improved. For example, due to the uniform connectivity, flow accumulation
372 is smoother in spatial transitions (Figure 9c and 11). Consequently, surface
373 runoff, evapotranspiration, infiltration and stream discharge will be improved
374 (Figure 14).

375 Last, comparisons of stream networks suggest that spatial resolution has
376 an impact on model performance. Our analysis shows that HexWatershed
377 performs much better at coarse resolutions.

378 Taken together, HexWatershed should be applied to hydrologic models
379 to improve hydrologic simulations.

380 6. Limitations

381 Based on our analysis, we have identified a few limitations in this study:

- 382 1. Currently a standard file format to manage HGSD based datasets is
383 unavailable. In this study, we rely on ESRI Shapefile for storage and
384 visualization. However, due to the limitations of Shapefile, we can use
385 NetCDF or HDF to improve performance. For example, NetCDF is
386 the file format currently used by MPAS mesh grid.
- 387 2. The HexWatershed model relies on the accuracy of DEM resampling.
388 There are challenges in converting SGSD based raster DEM to HGSD
389 based DEM. Currently we use the nearest resampling method because it
390 will not introduce new values into the system and it's computationally
391 efficient. Other advanced resampling methods should be used in the
392 future [13].
- 393 3. Our model currently only considers the steepest slope as the single
394 flow direction. In some scenarios, multiple flow directions should be
395 considered. And we can implement the D-infinity algorithm on the
396 HGSD method [12].
- 397 4. We didn't implement the stream "burn-in" capability in the current
398 version, which could further improve the performance under certain
399 circumstances [11].
- 400 5. Currently there is not a tool that can be used to convert existing SGSD
401 based datasets to the HGSD based format. But similar function is
402 already available in many coupled Earth system models. In the future,
403 we plan to provide a tool to resolve this limitation.

- 404 6. Currently we only ran HexWatershed model at 30 m , 90 m and 100 m
405 spatial resolutions. More simulations at different resolutions are needed
406 to evaluate the model sensitivity to spatial resolution.

407 **7. Conclusion**

408 We have developed a watershed delineation model (HexWatershed) using
409 the hexagon grid spatial discretization method. We have applied this model
410 to two different types of watersheds in the western US featuring steep and
411 flat terrain. Model outputs have shown that HexWatershed can reproduce
412 all the watershed delineation characteristics.

413 Comparisons between outputs from HexWatershed and the traditional
414 square grid spatial discretization method have shown that the HGSD method
415 has multiple advantages including removal of "island" effect and improvement
416 of flow direction and all watershed characteristics such as subbasin boundary
417 that depend on the flow direction because of the consistent connectivity.
418 Analysis also suggests that spatially distributed hydrologic simulations which
419 rely on connectivity/routing can be improved if the HGSD method is used.

420 Our model can be applied to continental or global scale to improve large
421 scale hydrologic simulations.

422 **8. Acknowledgement**

423 The research described in this paper was primarily funded by the Labo-
424 ratory Directed Research and Development (LDRD) Program Quickstarter
425 project 206583 at Pacific Northwest National Laboratory, a multiprogram
426 national laboratory operated by Battelle for the U.S. Department of En-
427 ergy. LRL was supported by U.S. Department of Energy Office of Science
428 Biological and Environmental Research through the Earth and Environmen-
429 tal System Modeling program as part of the Energy Exascale Earth System
430 Model (E3SM) project. The data used for model simulations are listed in the
431 tables and all input data and model outputs are archived on the computers at
432 PNNL and will be available by contacting Chang Liao (chang.liao@pnnl.gov).
433 The HexWatershed program can be accessed through Github [HexWatershed](#).
434 Some datasets in the Tin Pan watershed were produced from an effort of
435 hydrology-based design of geomorphic evapotranspiration covers for recla-
436 mation of mine land. A portion of this research was performed using PNNL
437 Research Computing at Pacific Northwest National Laboratory. PNNL is

438 operated for DOE by Battelle Memorial Institute under contract DE-AC05-
439 76RL01830.

440 **9. References**

- 441 [1] Richard Barnes. Parallel non-divergent flow accumulation for trillion
442 cell digital elevation models on desktops or clusters. *Environmental*
443 *Modelling & Software*, 92:202–212, 2017.
- 444 [2] Richard Barnes, Clarence Lehman, and David Mulla. Priority-flood: An
445 optimal depression-filling and watershed-labeling algorithm for digital
446 elevation models. *Computers & Geosciences*, 62:117–127, 2014.
- 447 [3] Colin P D Birch, Sander P Oom, and Jonathan A Beecham. Rectangular
448 and hexagonal grids used for observation, experiment and simulation in
449 ecology. *Ecological modelling*, 206(3-4):347–359, 2007.
- 450 [4] Luis de Sousa, Fernanda Nery, Ricardo Sousa, and Joao Matos. Assessing
451 the accuracy of hexagonal versus square tilled grids in preserving
452 DEM surface flow directions. In *7th international symposium on spatial*
453 *accuracy assessment in natural resources and environmental sciences*,
454 pages 191–200, 2006.
- 455 [5] Qiang Du, Max D Gunzburger, and Lili Ju. Voronoi-based finite volume
456 methods, optimal Voronoi meshes, and PDEs on the sphere. *Computer*
457 *methods in applied mechanics and engineering*, 192(35-36):3933–3957,
458 2003.
- 459 [6] ESRI and White PaperdJuly. ESRI shapefile technical description. *Com-*
460 *put. Stat*, 16:370–371, 1998.
- 461 [7] Antonio Francipane, Valeriy Y Ivanov, Leonardo V Noto, Erkan Istan-
462 bulluoglu, Elisa Arnone, and Rafael L Bras. tRIBS-Erosion: A parsimo-
463 nious physically-based model for studying catchment hydro-geomorphic
464 response. *Catena*, 92:216–231, 2012.
- 465 [8] Dean Gesch, Michael Omoen, Susan Greenlee, Charles Nelson, Michael
466 Steuck, and Dean Tyler. The national elevation dataset. *Photogram-*
467 *metric engineering and remote sensing*, 68(1):5–32, 2002.

- 468 [9] Brian Hamilton and Alberto Torin. Finite Difference Schemes on Hexagonal
469 Grids for Thin Linear Plates with Finite Volume Boundaries. In *DAFx*, pages 5–12. Citeseer, 2014.
- 471 [10] Arlen W Harbaugh. *MODFLOW-2005, the US Geological Survey modular ground-water model: The ground-water flow process*. US Department
472 of the Interior, US Geological Survey Reston, VA, USA, 2005.
- 474 [11] Ferdi Hellweger and D Maidment. AGREE-DEM surface
475 reconditioning system. *Online at <http://www.ce.utexas.edu/prof/maidment/gishydro/ferdi/research/agree/agree.html> (last accessed March 3, 2005)*, 1997.
- 478 [12] Wesley R Henson, Rose L Medina, C Justin Mayers, Richard G Niswonger, and R Steven Regan. *CRT–Cascade Routing Tool to define and
479 visualize flow paths for grid-based watershed models*. US Department of
480 the Interior, US Geological Survey, 2013.
- 482 [13] Innchyn Her and Chi-Tseng Yuan. Resampling on a pseudohexagonal
483 grid. *CVGIP: Graphical Models and Image Processing*, 56(4):336–347,
484 1994.
- 485 [14] Craig M Johnston, Thomas G Dewald, Timothy R Bondelid, Bruce B
486 Worstell, Lucinda D McKay, Alan Rea, Richard B Moore, and
487 Jonathan L Goodall. Evaluation of catchment delineation methods for
488 the medium-resolution national hydrography dataset. Technical report,
489 2009.
- 490 [15] Christian D Langevin, Joseph D Hughes, Edward R Banta, Richard G
491 Niswonger, Sorab Panday, and Alden M Provost. Documentation for
492 the MODFLOW 6 groundwater flow model. Technical report, 2017.
- 493 [16] Hongyi Li, Mark S Wigmosta, Huan Wu, Maoyi Huang, Yinghai Ke,
494 Andr M Coleman, and L Ruby Leung. A physically based runoff routing
495 model for land surface and earth system models. *Journal of Hydrometeorology*,
496 14(3):808–828, 2013.
- 497 [17] Chang Liao, Qianlai Zhuang, L Ruby Leung, and Laodong Guo. Quantifying
498 Dissolved Organic Carbon Dynamics Using a ThreeDimensional
499 Terrestrial Ecosystem Model at High SpatialTemporal Resolutions.
500 *Journal of Advances in Modeling Earth Systems*.

- 501 [18] Steven L Markstrom, Richard G Niswonger, R Steven Regan, David E
502 Pradic, and Paul M Barlow. *GSFLOW, Coupled Ground-Water and*
503 *Surface-Water Flow Model Based on the Integration of the Precipitation-*
504 *Runoff Modeling System (PRMS) and the Modular Ground-Water Flow*
505 *Model (MODFLOW-2005)*. US Department of the Interior, US Geolog-
506 ical Survey, 2008.
- 507 [19] Reed M Maxwell, Stefan J Kollet, Steven G Smith, Carol S Woodward,
508 Robert D Falgout, Ian M Ferguson, Chuck Baldwin, William J Bosl,
509 Richard Hornung, and Steven Ashby. ParFlow users manual. *Inter-*
510 *national Ground Water Modeling Center Report GWMI*, 1(2009):129,
511 2009.
- 512 [20] S Neitsch, J Arnold, J Kiniry, J R Williams, and K W King. SWAT2009
513 Theoretical Documentation. *Texas Water Ressources Institute Technical*
514 *Report*, (406), 2005.
- 515 [21] Olivier Planchon and Frdric Darboux. A fast, simple and versatile algo-
516 rithm to fill the depressions of digital elevation models. *Catena*, 46(2-
517 3):159–176, 2002.
- 518 [22] Yizhong Qu. *An integrated hydrologic model for multi-process simula-*
519 *tion using semi-discrete finite volume approach*. The Pennsylvania State
520 University, 2005.
- 521 [23] David A Randall, Todd D Ringler, Ross P Heikes, Phil Jones, and John
522 Baumgardner. Climate modeling with spherical geodesic grids. *Com-*
523 *puting in Science & Engineering*, 4(5):32–41, 2002.
- 524 [24] H Renssen and J M Knoop. A global river routing network for use in
525 hydrological modeling. *Journal of Hydrology*, 230(3-4):230–243, 2000.
- 526 [25] K Sahr. DGGRID version 6.2 b: User documentation for discrete global
527 grid software, 2015.
- 528 [26] Kevin Sahr. Hexagonal discrete global grid systems for geospatial com-
529 puting. *Archiwum Fotogrametrii, Kartografii i Teledetekcji*, 22:363–376,
530 2011.

- 531 [27] Kevin Sahr. Central Place Indexing: Hierarchical Linear Indexing Sys-
532 tems for Mixed-Aperture Hexagonal Discrete Global Grid Systems. *Car-*
533 *tographica: The International Journal for Geographic Information and*
534 *Geovisualization*, 54(1):16–29, 2019.
- 535 [28] David G Tarboton. A new method for the determination of flow direc-
536 tions and upslope areas in grid digital elevation models. *Water resources*
537 *research*, 33(2):309–319, 1997.
- 538 [29] David G Tarboton, Rafael L Bras, and Ignacio RodriguezIturbe. On the
539 extraction of channel networks from digital elevation data. *Hydrological*
540 *processes*, 5(1):81–100, 1991.
- 541 [30] Teklu K Tesfa, H-Y Li, L R Leung, Maoyi Huang, Yinghai Ke, Yu Sun,
542 and Ying Liu. A subbasin-based framework to represent land surface
543 processes in an Earth system model. *Geoscientific Model Development*,
544 7(3):947–963, 2014.
- 545 [31] Teklu K Tesfa, L Ruby Leung, Maoyi Huang, HongYi Li, Nathalie
546 Voisin, and Mark S Wigmosta. Scalability of gridand subbasinbased
547 land surface modeling approaches for hydrologic simulations. *Journal of*
548 *Geophysical Research: Atmospheres*, 119(6):3166–3184, 2014.
- 549 [32] Lei Wang and Hongxing Liu. An efficient method for identifying and
550 filling surface depressions in digital elevation models for hydrologic anal-
551 ysis and modelling. *International Journal of Geographical Information*
552 *Science*, 20(2):193–213, 2006.
- 553 [33] Lu Wang and Tinghua Ai. The comparison of drainage network ex-
554 traction between square and hexagonal grid-based dem. *International*
555 *Archives of the Photogrammetry, Remote Sensing & Spatial Information*
556 *Sciences*, 42(4), 2018.
- 557 [34] Hilary Weller, John Thuburn, and Colin J Cotter. Computational modes
558 and grid imprinting on five quasi-uniform spherical C grids. *Monthly*
559 *Weather Review*, 140(8):2734–2755, 2012.
- 560 [35] Hilary Weller, Henry G Weller, and Aim Fournier. Voronoi, Delaunay,
561 and block-structured mesh refinement for solution of the shallow-water
562 equations on the sphere. *Monthly Weather Review*, 137(12):4208–4224,
563 2009.

- 564 [36] M Winchell, R Srinivasan, M Di Luzio, and J Arnold. ArcSWAT inter-
565 face for SWAT 2005. *Users Guide, Blackland Research Center, Texas*
566 *Agricultural Experiment Station, Temple, 2007.*

⁵⁶⁷ **Appendix A. Model Structure**

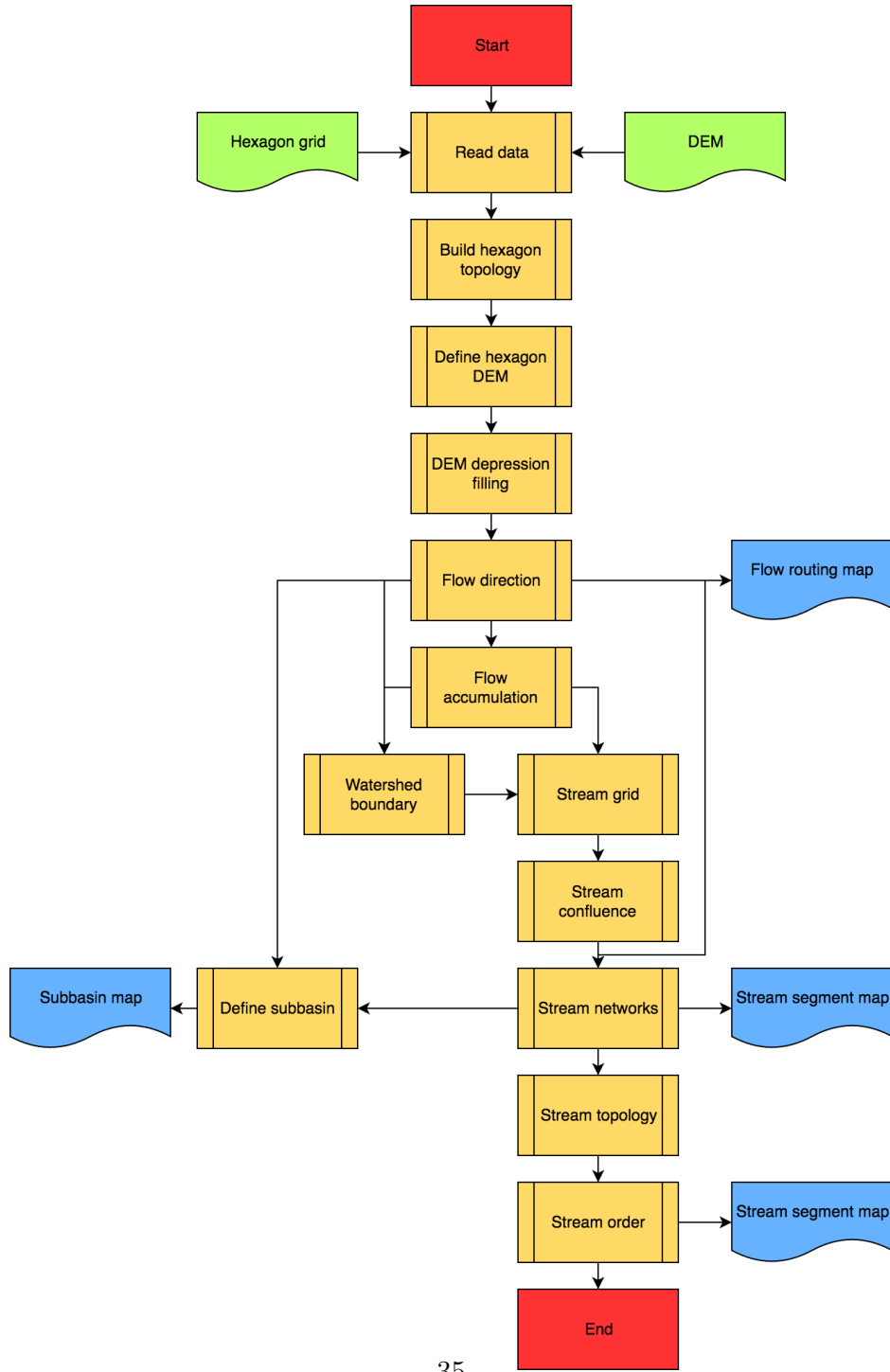


Figure A.15: The work flow of the HexWatershed model. The red tiles are start and end. The yellow tiles are processing steps. The green and blue tiles are major model inputs and outputs, respectively.

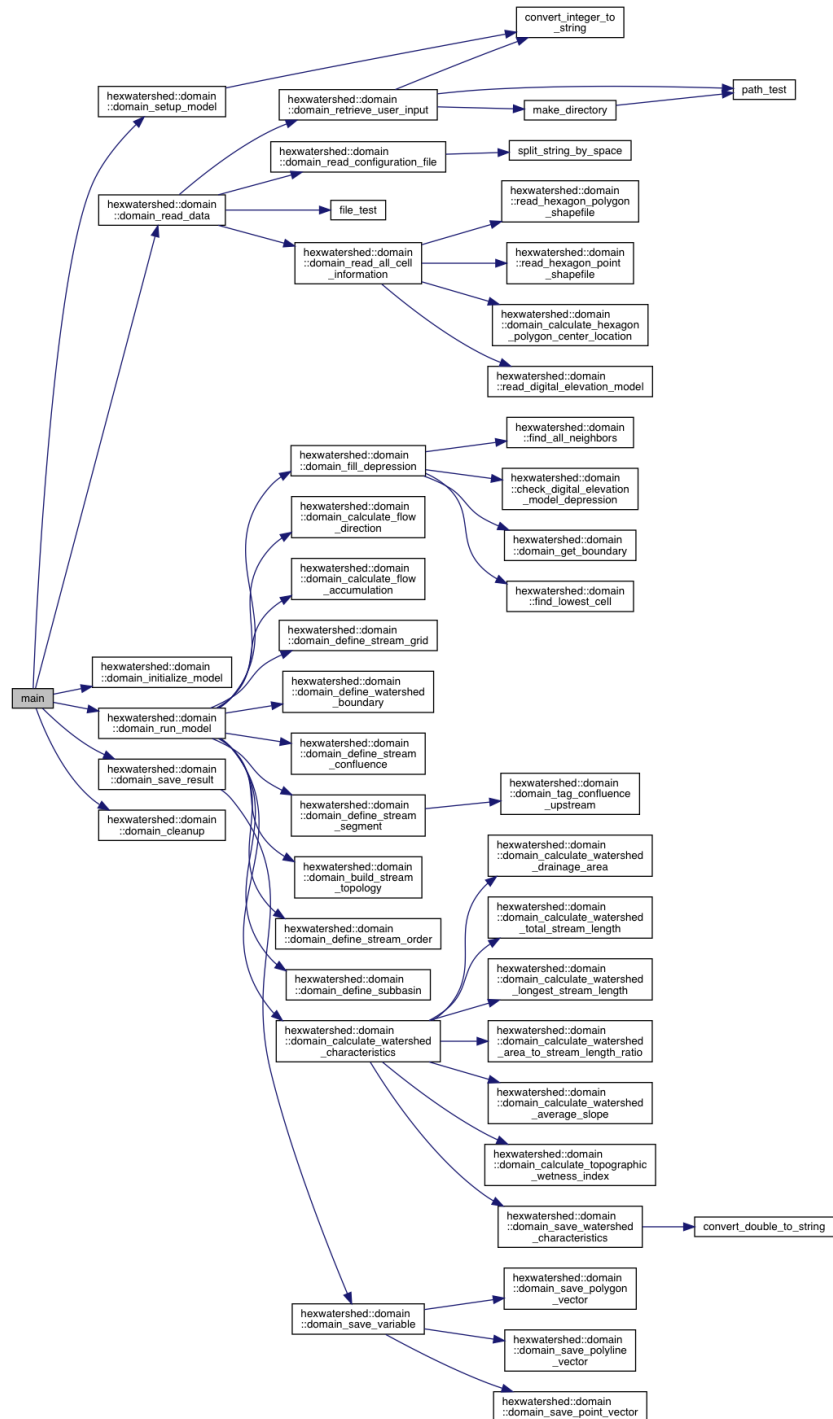


Figure A.16: The structure of HexWatershed model generated by Doxygen.

568 **Appendix B. Depression Filling**

- 569 1. Find the boundary of the grid system and push them into a queue Q;
570 2. Find the grid A which has the lowest elevation in Q;
571 3. Find all the untreated neighbors of grid A and put them into array B;
572 4. If any member of B has a lower elevation than A, increase its elevation
573 to higher than A's;
574 5. Push B into Q and remove A from Q;
575 6. If there are still untreated grids, go to step 2.

576 **Appendix C. Flow Accumulation**

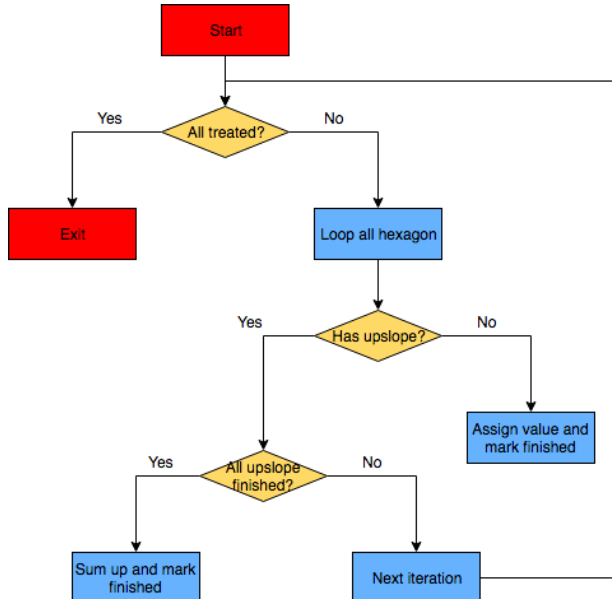


Figure C.17: Illustration of the flow accumulation algorithm. In a hexagon grid system, this algorithm loops through grids using the global IDs and calculates accumulation once its upslope accumulations are finished.

⁵⁷⁷ **Appendix D. Model Results**

⁵⁷⁸ *Appendix D.1. Tin Pan*

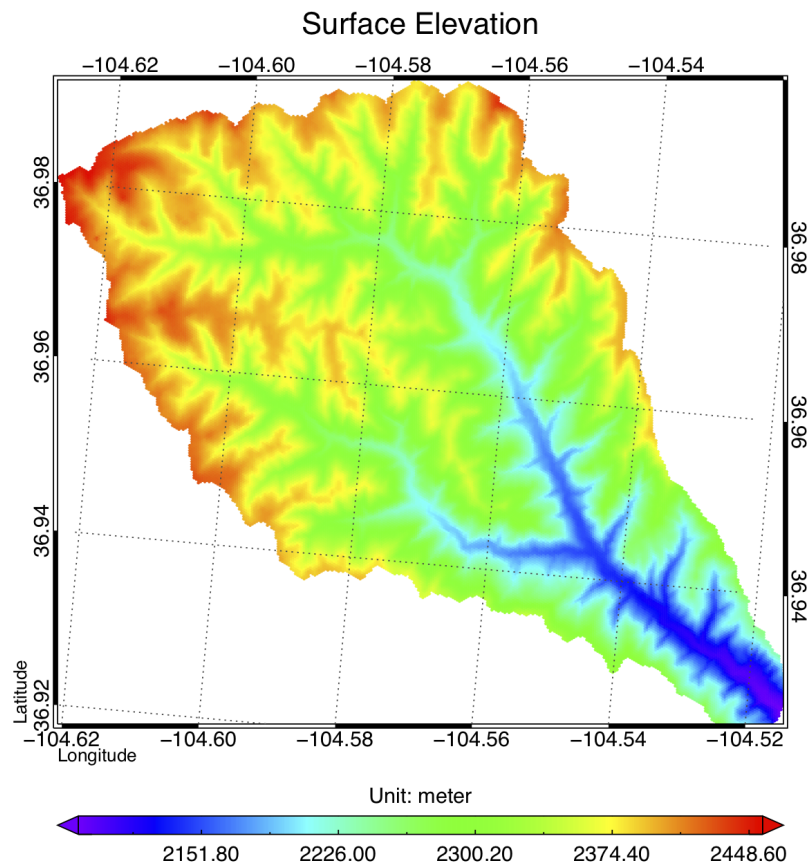


Figure D.18: The digital elevation model using the HGSD method (m).

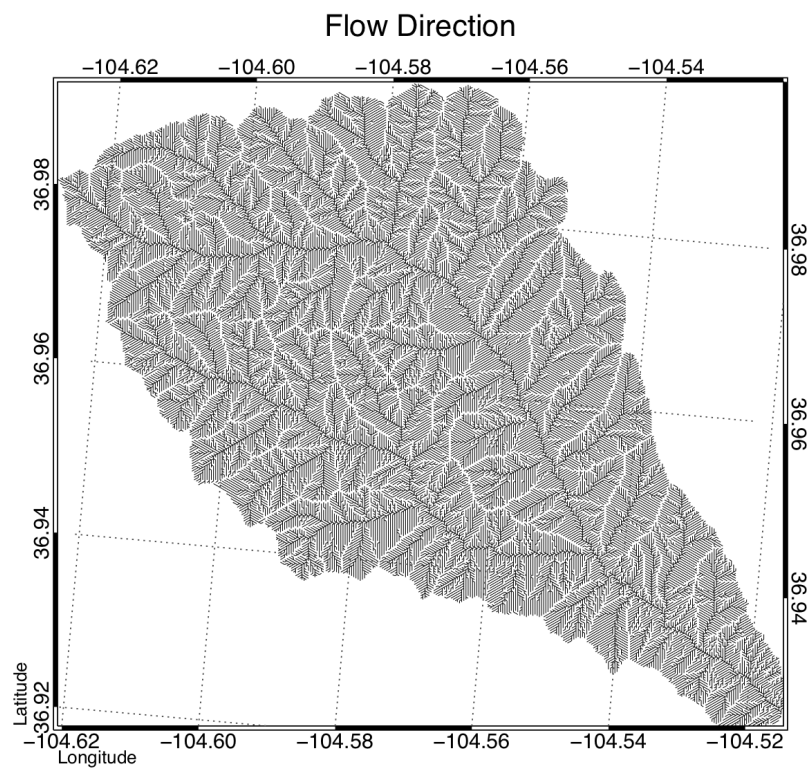


Figure D.19: The spatial distribution of simulated flow direction.

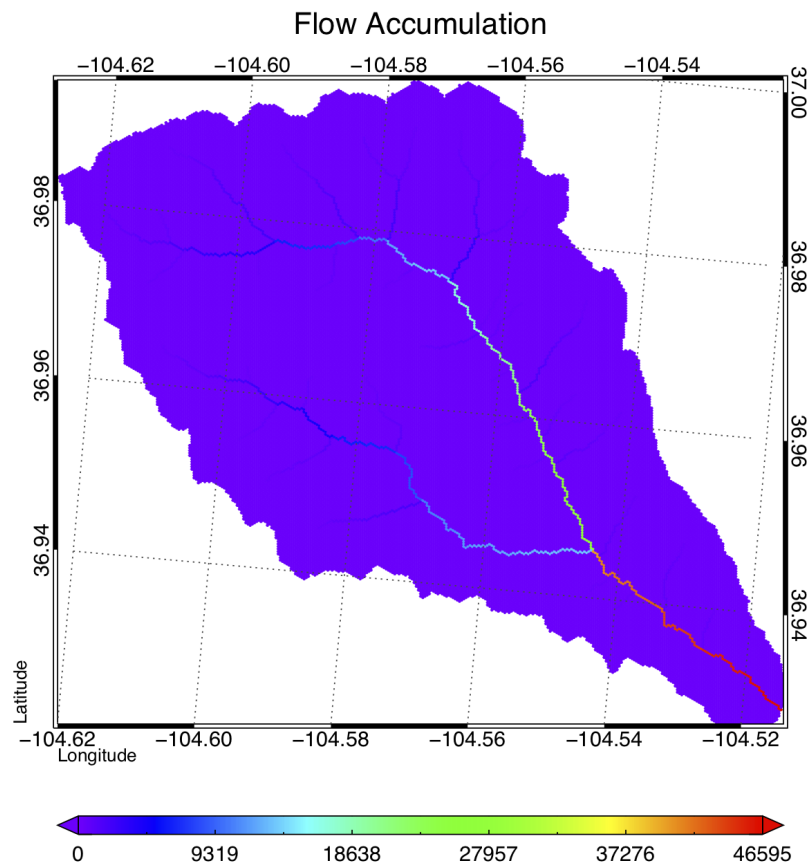


Figure D.20: The spatial distribution of simulated flow accumulation.

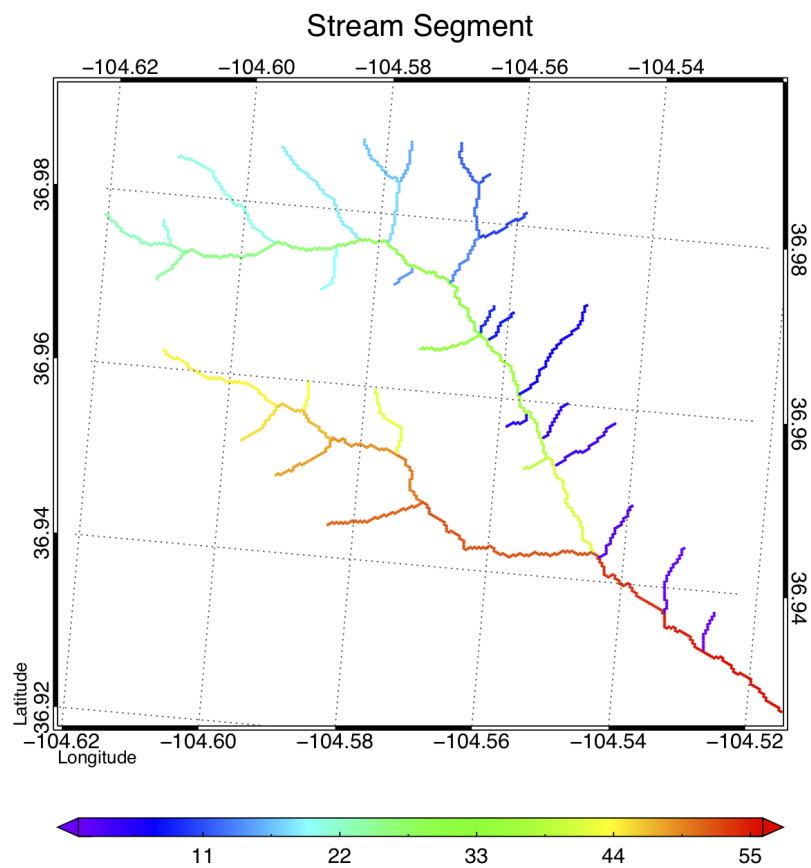


Figure D.21: The spatial distribution of simulated stream networks.

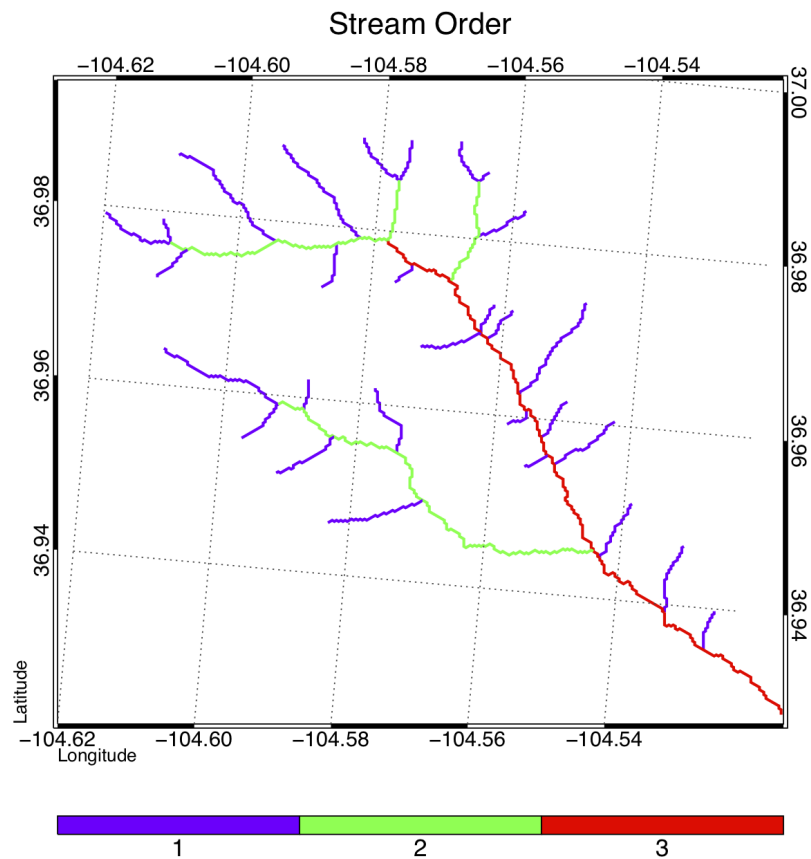


Figure D.22: The spatial distribution of simulated stream order.

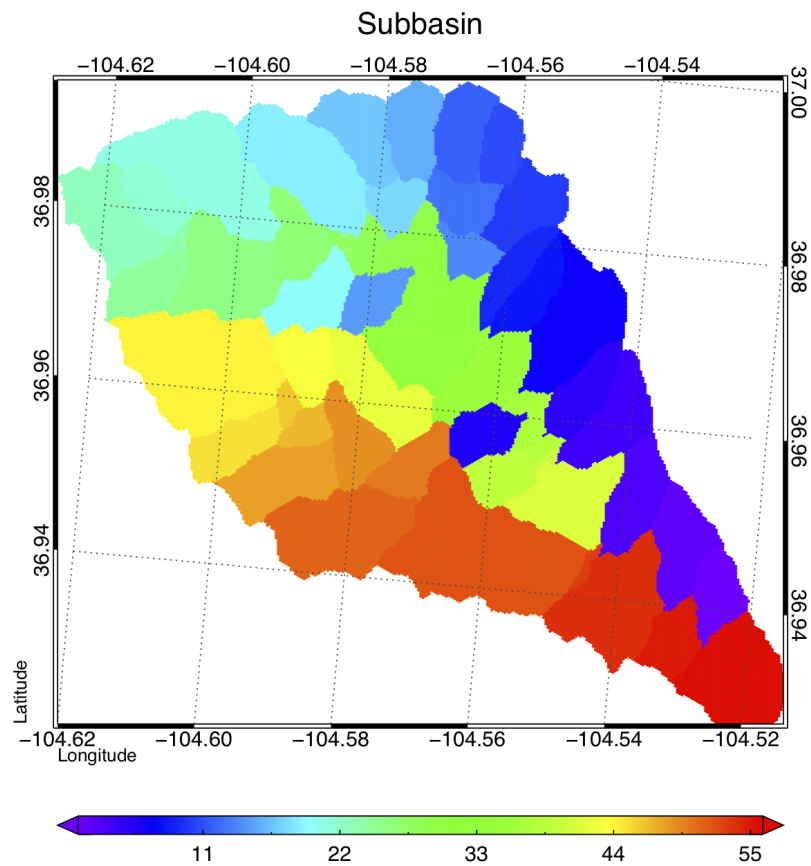


Figure D.23: The spatial distribution of simulated subbasin boundary. The colored polygons represent hexagons in the same subbasin.

⁵⁷⁹ Appendix D.2. Columbia Basin Flat

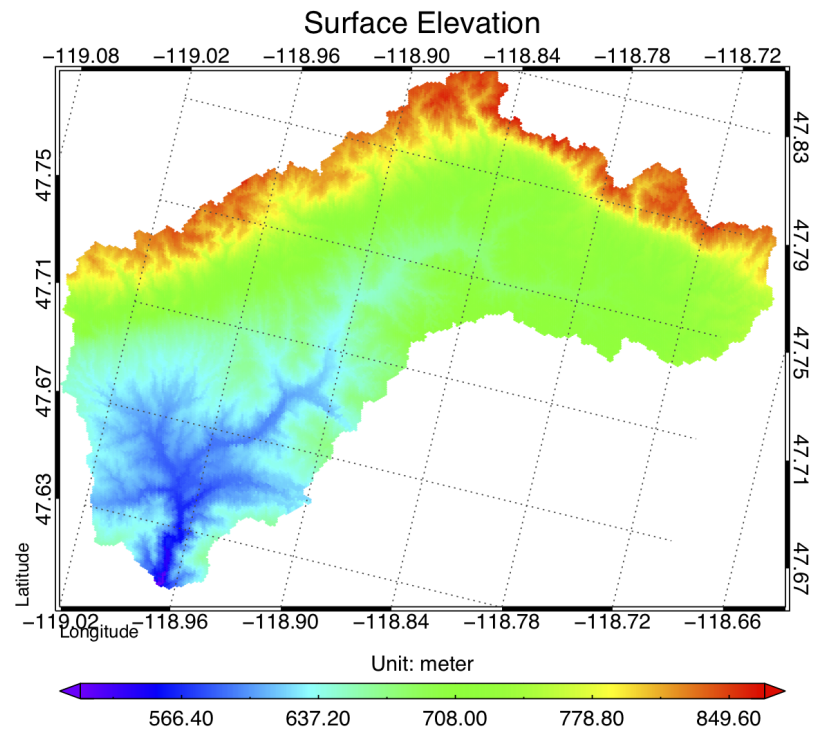


Figure D.24: The digital elevation model using the HGSD method (m).

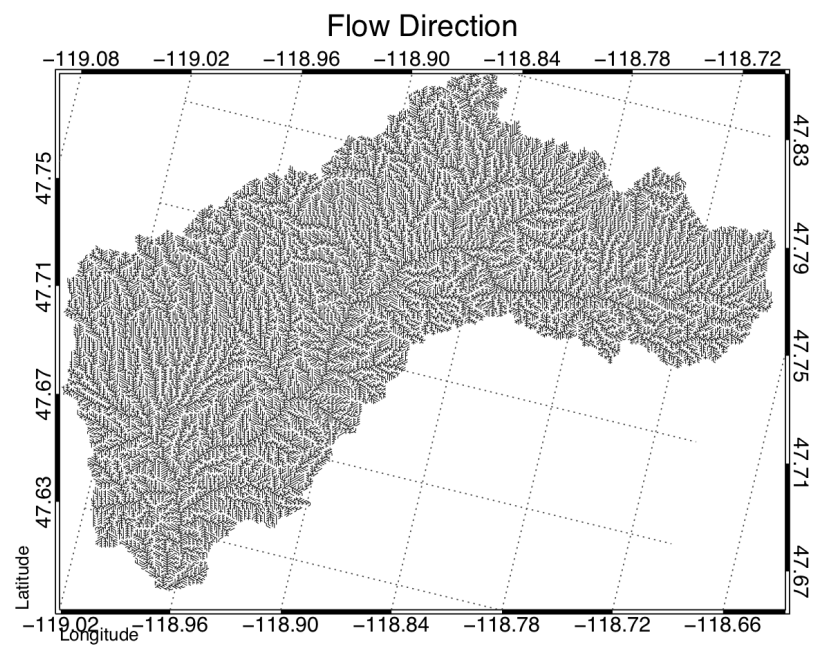


Figure D.25: The spatial distribution of simulated flow direction.

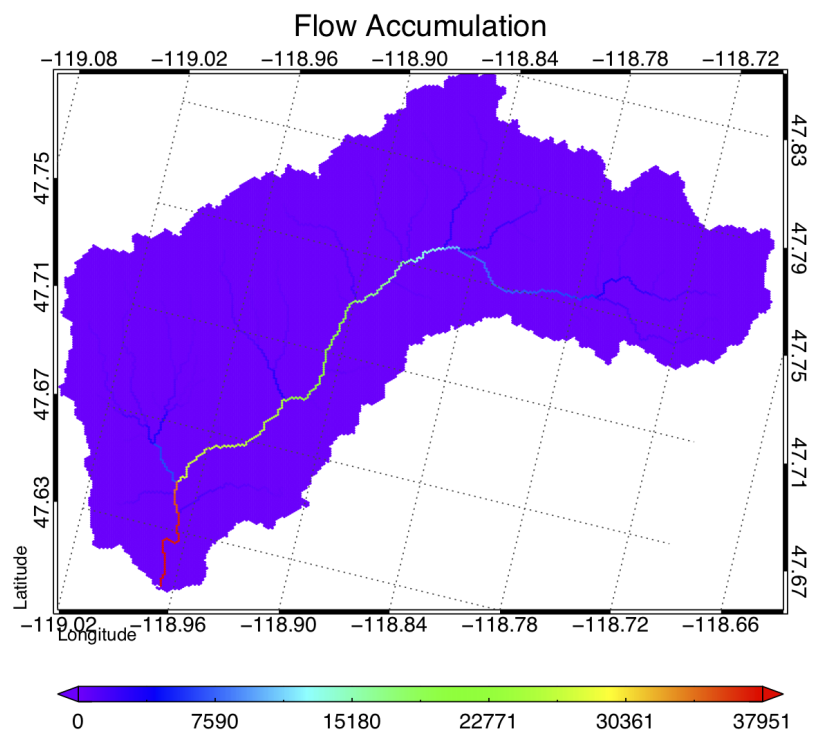


Figure D.26: The spatial distribution of simulated flow accumulation.

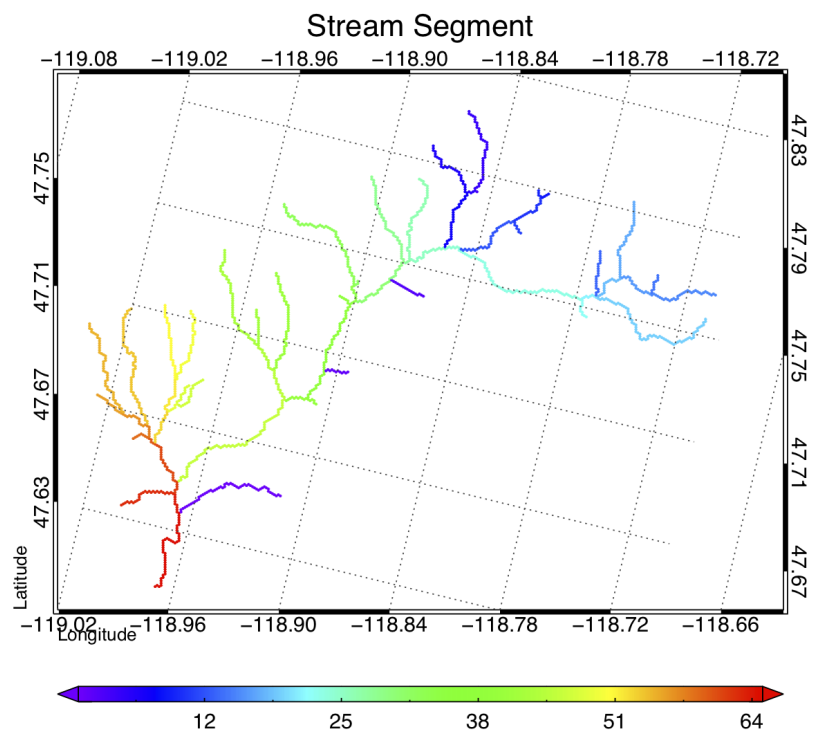


Figure D.27: The spatial distribution of simulated stream networks.

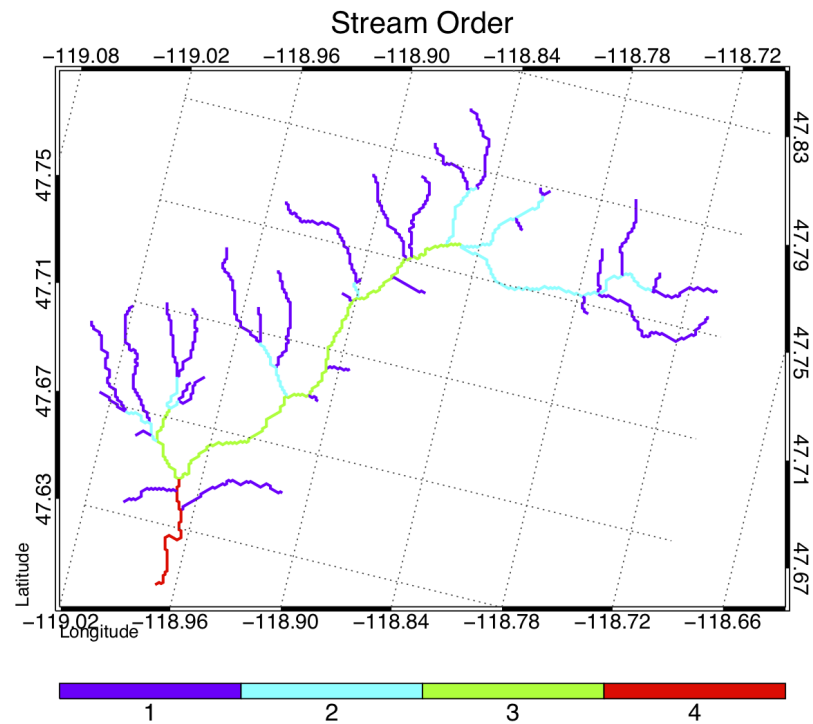


Figure D.28: The spatial distribution of simulated stream order.

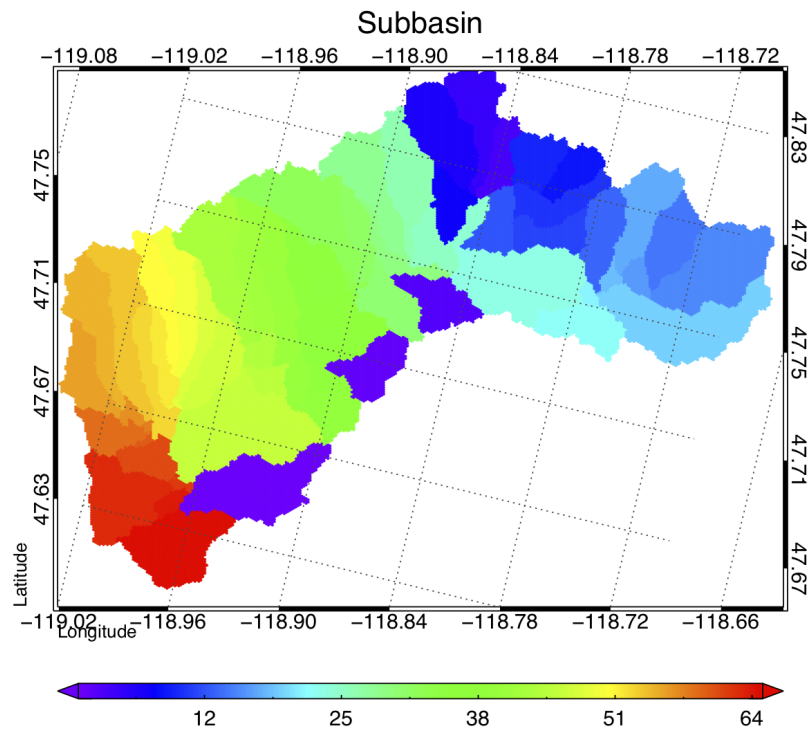


Figure D.29: The spatial distribution of simulated subbasin boundary. The colored polygons represent hexagons in the same subbasin.